MICROSTRUCTURAL ANALYSIS OF BONE OF THE SAUROPOD DINOSAUR *SEISMOSAURUS* BY TRANSMISSION ELECTRON MICROSCOPY

by THOMAS G. ZOCCO *and* HILDE L. SCHWARTZ

ABSTRACT. Transmission electron microscopy (TEM) is commonly used to characterize materials with respect to crystal structure, chemical composition, defect density and type, as well as other microstructural features. Observation of bone from the Upper Jurassic sauropod dinosaur *Seismosaurus* using this technique, reveals a unique bimodal crystallite structure which appears to have local preferred orientation. Most crystallites are small oblong grains, averaging approximately 100 nm long and 20 nm wide; larger hexagonal crystallites are also present, ranging from 80 to 400 nm in diameter. The larger crystallites are found near naturally occurring canals and pores in the *Seismosaurus* bone. Electron diffraction and chemical analyses show that both the small and large crystallites are composed of fluorapatite. Comparative analyses of *Seismosaurus* with modern crocodile, Pleistocene mammoth, and Cretaceous theropod dinosaur bones show that younger fossil bone microstructure is essentially unaltered; the older fossil bones share a unique crystalline microstructure in which original and diagenetic apatite is intermixed.

BONE is an abundant and important component of the fossil record. Historically, research on the changes that occur in bone with burial and time has focused on mineralogy and histology, which relate to fluorine dating, diagenetic, and palaeoecological studies. This work has led to recognition of some general aspects of bone fossilization, including: (1) alteration of original bone apatite, generally carbonate hydroxyapatite ($Ca_5(PO_4,CO_3)_3(Cl,OH,F)_2$) to carbonate fluorapatite ($Ca_5(PO_4,CO_3)_3F_2$); (2) selective isomorphous substitution of certain elements (e.g. fluorine, uranium, rare earth elements) and the loss of others (e.g. nitrogen) from bone mineral; (3) the gradual loss of organic matter from bone matrix; and (4) the introduction of new mineral phases into pores and interstices left vacant by the removal of organic material. It has been known for more than a century that much, if not most, fossil bone is composed of either carbonate hydroxyapatite or its isostructural counterpart, carbonate fluorapatite (Middleton 1844; Carnot 1893). However, it is not known whether fossil bone apatite is original material or recrystallized.

Along with mineralogy, the crystalline ultrastructure of fossil bone is a key to understanding how and to what extent the fossils are changed from their primary state. In modern mammal bone, the crystallite constituents of bone apatite vary in size from 10 to 400 nm in length and width and 1 to 7·5 nm in thickness (Fitton Jackson and Randall 1956; Engstrom 1960; Cameron 1972). Variation in crystallite size occurs between different species (Osmund and Sawin 1959; Tannenbaum and Termine 1965), between different bones in the same animal and in different regions of the same bone (Robinson and Cameron 1964), and within living bone with age and/or fluorine uptake (Zipkin *et al.* 1962; Robinson and Cameron 1964; Eanes 1965; Posner *et al.* 1965; Tannenbaum and Termine 1965; Simpson 1966). Scanning electron microscopy (SEM) analyses of modern mammal bone show that the crystallites are rod-, needle- or tablet-shaped (Neuman and Neuman 1958; Robinson and Cameron 1964; Cameron 1972) and are aligned more or less parallel to collagen fibrils (e.g. Fernandez-Moran and Engstrom 1957; Eanes 1965). The extremely small size of bone apatite crystallites gives them large surface areas of 100–200 m^2/g (Engstrom 1972).

Few studies have looked at the comparative physical ultrastructure of fossil bones, but Jaffe and Sherwood (1951), Osmund and Sawin (1959), Brophy and Hatch (1962), Wyckoff *et al.* (1963),

[Palaeontology, Vol. 37, Part 3, 1994, pp. 493–503]

Lozinski (1973), and Tuross *et al.* (1989) used X-ray diffraction and/or powder X-ray photography to document changes in the sizes of apatite crystallites and unit cell parameters in fossil bone. Taken together, their results are contradictory and do not establish a model for change in bone apatite with time. Wyckoff *et al.* (1963), Wyckoff and Doberenz (1965), Wyckoff (1972), Tuross *et al.* (1980), and Wyckoff (1980) recorded good preservation of both organic and inorganic bone matrix in fossils using SEM and microradiographic images.

Surprisingly, transmission electron microscopy (TEM) has rarely been employed in studies of fossil ultrastructure, despite its wide use in biological ultrastructure and materials microstructure research. TEM allows simultaneous high magnification observation and high spatial resolution chemical analyses, which is advantageous over the more common scanning electron microscopy. Most of the studies which do include TEM analysis of fossils, look at histology and organic structure (ultrastructure), rather than inorganic mineral structure (e.g. Shackleford and Wyckoff 1964; Doberenz and Wyckoff 1967; Pawlicki 1978; Towe 1980), with the exception of Wyckoff (1972).

We originally examined inorganic structure (microstructure), and composition of a well-preserved fragment of the ischium from the Jurassic of the dinosaur *Seismosaurus* of New Mexico, using TEM in order to determine the presence and/or extent of recrystallization within the bone, and thus determine its degree of originality. *Seismosaurus* is a large sauropod dinosaur recently described by Gillette (1991). It belongs to the Diplodocidae and is known from the partial skeleton of one individual recovered from the Brushy Basin Member of the Morrison Formation (Schwartz and Manley 1992). The unexpected and unusual ultrastructure of *Seismosaurus* bone led us to a comparative examination of three other samples: a limb bone fragment from the Cretaceous theropod dinosaur, (probably *Albertosaurus*) (from Alberta, Canada); a limb fragment from a Late Pleistocene mammoth (from central Utah); and a scute from a recent crocodile (from Kenya) (Table 1). The theropod and crocodile specimens were collected and identified by the second author; the

TABLE 1. List of one specimens analysed by TEM for this study.

Specimen taxon	Skeletal part	Age
Crocodile	Scute	Recent
Mammoth	Limb fragment	Late Pleistocene
Albertosaurus dinosaur	Limb fragment	Cretaceous (c. 100 Ma)
Seismosaurus dinosaur	Ischium	Jurassic (154 ± 2·4 Ma – Woldegabriel and Hagan, work in preparation)

mammoth bone was collected and identified by D. D. Gillette. These specimens were chosen in order to test whether the *Seismosaurus* ultrastructure is a general characteristic of long-term bone diagenesis or a more specific characteristic of either reptile bone or the bone of large land-living animals.

EXPERIMENTAL PROCEDURE

Minerals such as apatite are fragile when extremely thin, and therefore, care must be taken in the preparation process to limit the amount of specimen handling. Several preparation methods were used to produce good quality TEM specimens; to produce a TEM specimen which is of any use, the thickness of the specimen in the observation area cannot exceed several hundred nanometers.

The first method involved the use of mortar and pestal to grind the bulk pieces into a fine powder which was then ultrasonically dispersed in hexane. A TEM grid coated with carbon was then dipped into the dispersion, dried, and examined in the microscope. Small pieces of bone were commonly found lying on the carbon film. These bone fragments were typically electron transparent, allowing

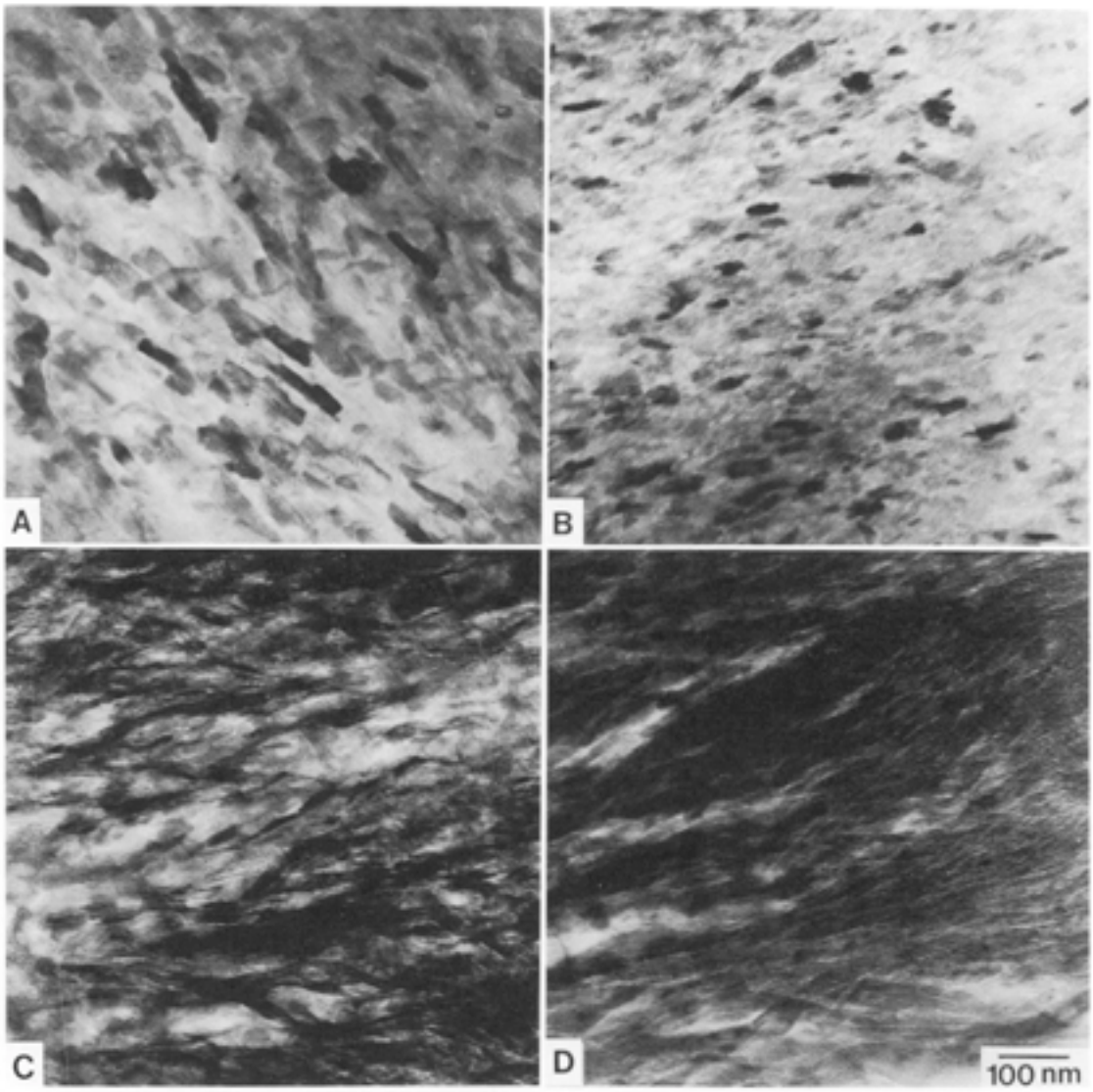

TEXT-FIG. 1. TEM images of representative bone apatite structure. A, *Seismosaurus*; B, theropod dinosaur; C, mammoth; D, crocodile. Note collagen fibrils in the younger bones.

both chemical and crystallographic information to be obtained, as well as direct microstructural examination.

The second method of specimen preparation preserved the natural structure of the fossilized bone and surrounding minerals by not requiring complete grinding of the bulk sample. Here the bulk sample was cut into slices which were thinned by grinding on SiC paper to a thickness of approximately 100 μm. These thin slices were then core-drilled using an ultrasonic drill with a 3 mm diameter bit. Careful handling became critical at this point, requiring vacuum tweezers to be used at all times.

Once the specimens were thinned and core-drilled, they were placed in an instrument which produced (by grinding using diamond paste) a small indent (dimple) in the specimen with a

thickness of approximately 10 μm. The specimen was then ion-thinned at liquid nitrogen temperatures using argon gas at 6 kV and a 15° grazing angle until a small perforation appeared. Thinning at low temperatures helped reduce chemical migration, microstructural modifications, and knock-on damage caused by the high energy bombarding argon atoms. The dimple provided a prethinned region of the disk to minimize ion thinning time and to improve the resulting electron transparent area for TEM observation.

Examination of the specimens was performed using a JEOL 2000EX Scanning Transmission Electron Microscope equipped with a Tracor Northern Energy Dispersive Spectrometry (EDS) system. A liquid nitrogen cold stage was used to minimize electron beam damage and contamination during observation and chemical analysis.

Prepared specimens are currently stored in the Materials Division, Materials Research and Processing Science Group of Los Alamos National Laboratory, USA.

RESULTS AND DISCUSSION

Ultrastructure

TEM observation of the various bones show several distinct differences, including a variation in crystal structure between the younger and older bones, a difference in crystallite size between bones as well as within some bones, and the presence or absence of collagen fibrils. Chemical variations also existed between the bones depending on the specific intruding ionic species found in the surrounding sediment. Text-figure 1A–D shows the typical ultrastructures observed in the *Seismosaurus*, theropod dinosaur, mammoth, and crocodile, respectively. The mammoth and crocodile bones show a dense arrangement of more-or-less uniform apatite crystallites oriented parallel to a network of collagen fibrils. These crystallites are more obvious in the mammoth bone, possibly due to initial disintegration of the organic matter in the fossil.

In contrast, the *Seismosaurus* and theropod dinosaur bones show no remaining traces of collagen and include two different types of crystallites differentiated by crystal size and shape. The majority of the bone is composed of fine, oblong-shaped crystallites ranging in size from 20–30 nm wide and up to 150 nm long. Other areas contain larger crystallites which are blocky plate-shaped, and range from 50–400 nm in width and length.

X-ray and electron diffraction

The bimodality of crystallite sizes in the dinosaur bones is easily recognized through direct observation, such as TEM or SEM imaging, X-ray diffraction (XRD) is also commonly used to measure indirectly bone crystal size, however XRD averages overall crystal size and thus cannot recognize discrete size groups easily.

X-ray diffraction of the four fossil bones studied in this investigation shows that the older bones (*Seismosaurus* and theropod dinosaur) are composed of fluorapatite, while the younger mammoth and crocodile bones are composed of hydroxyapatite.

Text-figure 2A–D shows electron diffraction patterns from fine crystalline regions (shown in Text-fig. 1), for *Seismosaurus*, the theropod dinosaur, mammoth, and crocodile, respectively. Analysis of the *Seismosaurus* and theropod diffraction patterns match what would be expected for a calcium fluoride phosphate and francolite mixture. The ratio of minerals is unknown. Electron microprobe analysis of *Seismosaurus* bone (Schwartz and Snow, work in preparation) indicates that it contains as much as 3·9 weight per cent fluorine. The patterns from the mammoth and crocodile give a reasonable fit to hydroxyapatite, as might be expected. These mineralogies are consistent with the common assumption that all fossil bone was formed originally of dahllite (carbonate hydroxyapatite), changing to francolite (carbonate fluorapatite) with time.

Diffuseness of the rings in the electron diffraction patterns from the younger bones may be due to the presence of a large proportion of organic material and/or to the presence of extremely fine crystallite sizes. A range of crystallite sizes is present in any one bone (Robinson and Cameron

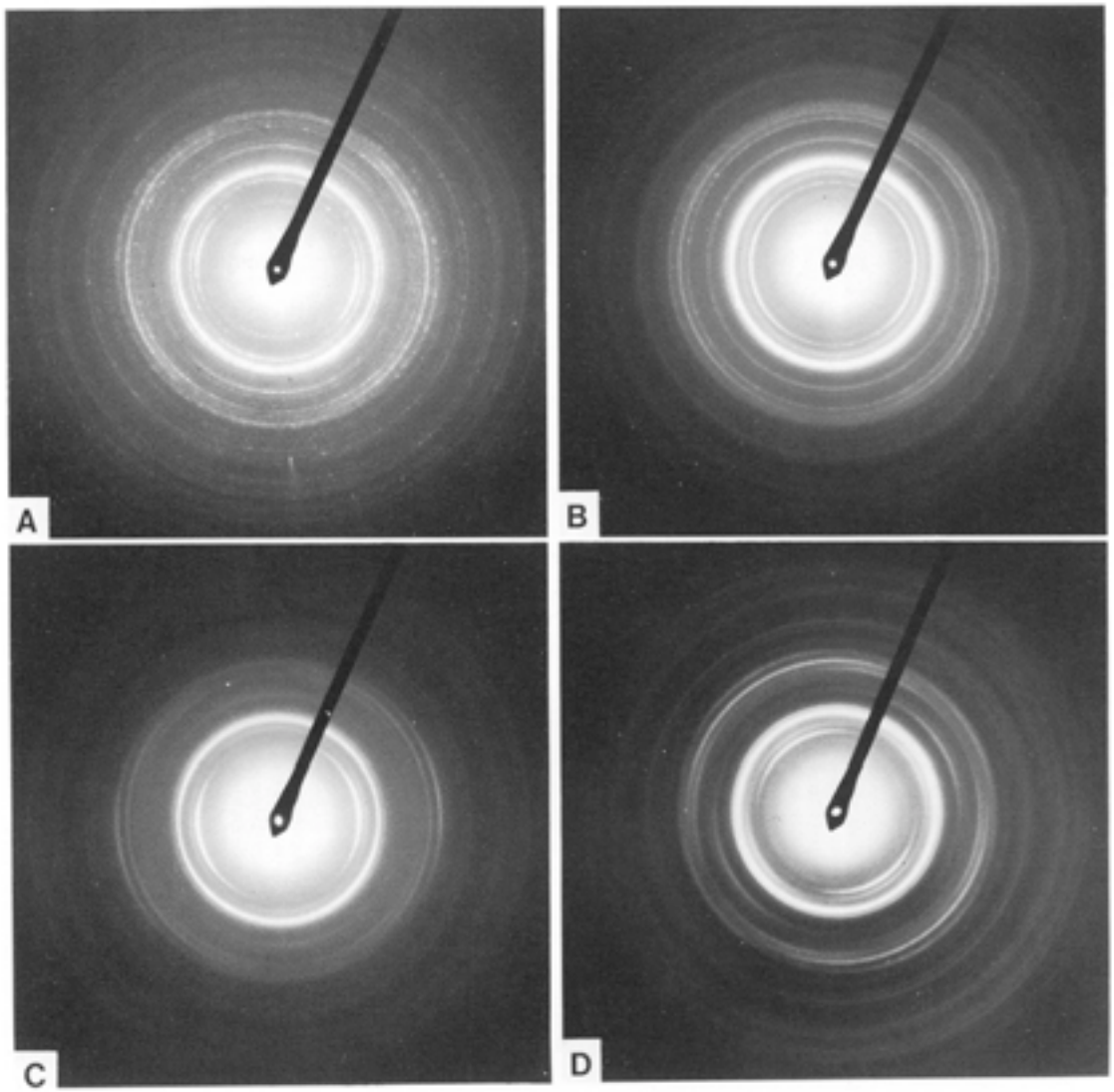

TEXT-FIG. 2. Electron diffraction patterns taken from large clusters of apatite crystals. A, *Seismosaurus*; B, theropod dinosaur; C, mammoth; and D, crocodile bones. Partial diffraction rings indicate some degree of preferred orientation in all the fossil bones examined.

1964); the absence of the finer fraction of crystallites in fossils or sub-fossils, due to dissolution or washing out with the breakdown of organic matter (Tuross *et al.* 1989), would not be surprising.

Text-figure 3A illustrates a possible crystallographic shape of the hexagonal crystals (Cuisinier *et al.* 1987). Close examination of the crystallites present in the younger bones shows that they are oriented with their long axes parallel to the long direction of the collagen fibrils. Diffraction pattern analysis (Eddington 1976) suggests the (0001) basal planes of the hexagonal structure lie perpendicular to the length of the fibril. This is illustrated in Text-figure 3B–C, where the (0002) planes produce partial diffraction rings. Full diffraction rings indicate a random orientation. Each ring or partial ring represents a specific plane normal in the crystal structure (these are represented

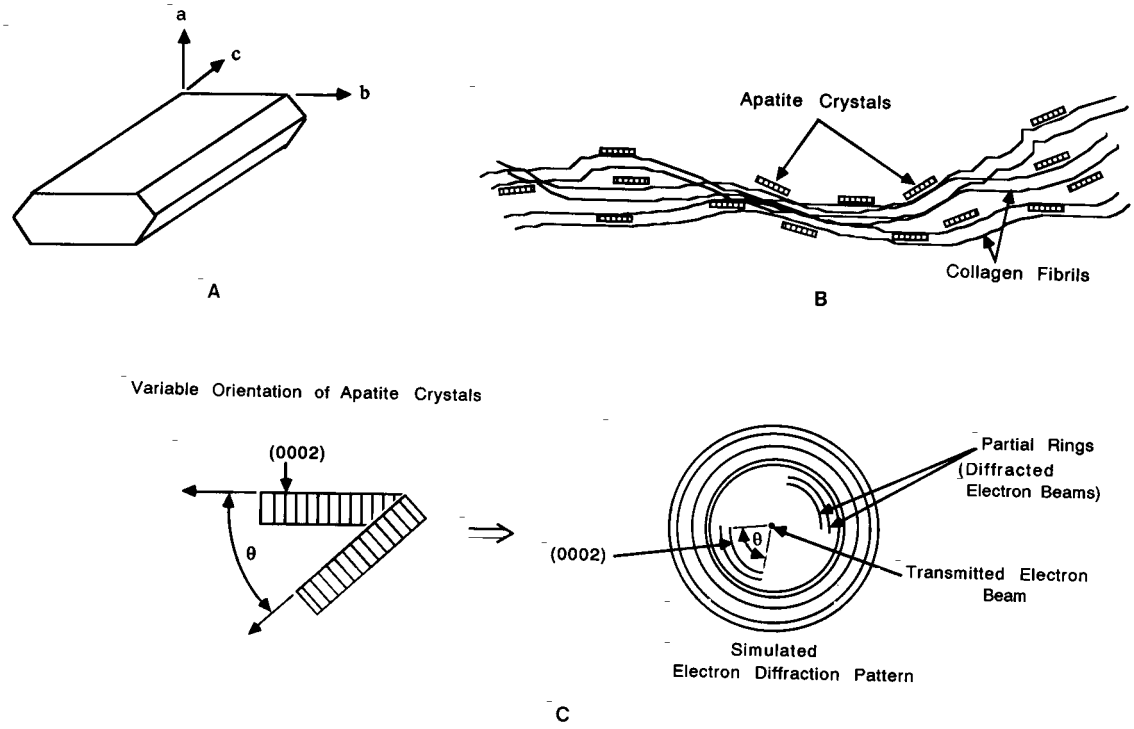

TEXT-FIG. 3. A, Schematic representation of one possible form of the hexagonal apatite crystals; both rod and plate shapes exist. B, schematic of apatite crystals lying parallel to collagen fibrils; basal planes (0001) lie perpendicular to the long axes of the crystals and collagen fibrils. C, diagram illustrating the effect of preferred orientation of apatite crystallites on the resulting electron diffraction pattern; partial diffraction rings occur with an angular relationship equal to the angular orientation range of the apatite crystals; (0002) planes are used because (0001) planes are symmetry extinct in the true diffraction pattern.

as peaks in XRD). The partial diffraction ring is produced with an arc (over the angle θ) which follows the orientation of the crystallites as they emulate the natural curvature of the collagen fibrils. This preferred orientation is also found in the older bones, indicating there may have been a similar preferred orientation apatite growth behaviour.

Nucleation and growth of apatite crystals

The presence of a bimodal size distribution of crystallites in the older fossils (Text-fig. 4) as compared to more recent bones shows that this peculiar ultrastructure is not a general characteristic of either reptiles or large land-living animals, and questions the similarity of bone growth in dinosaurs versus present-day animals. It is possible that dinosaur bones had unique ultrastructural features, but it seems unlikely given the relatively conservative nature of bone and skeletal evolution. A more probable scenario is that the original dinosaur ultrastructure has been modified by diagenetic processes during the millenia these bones have existed.

Electron diffraction pattern analysis (Text-fig. 2) and chemical analysis (Text-fig. 5) confirm the presence of fluorapatite crystals approximately 20 nm in length in *Seismosaurus* bone. Larger apatite crystals are also present. The larger crystallites tend to be clustered near cracks and pore spaces within the bones (Text-fig. 6). This arrangement, along with their conspicuously greater size and euhedral appearance, suggests that the larger crystallites grew under a different set of conditions

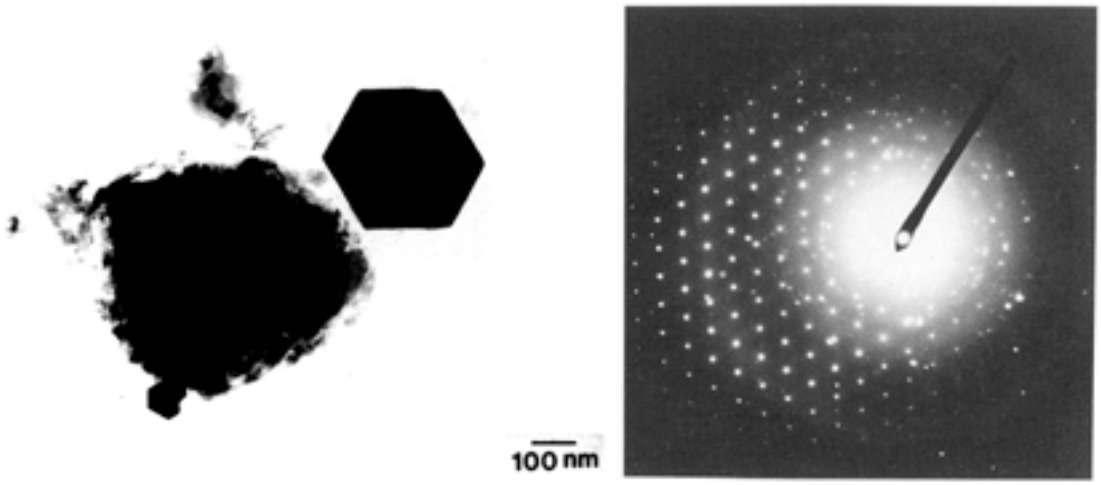

TEXT-FIG. 4. A, TEM micrograph of a region of fine apatite crystallites and a large apatite crystal exhibiting hexagonal shape (*Seismosaurus* bone). B, electron diffraction pattern of A showing the polycrystalline pattern, as well as the single crystal pattern as viewed along the c-axis, [0001].

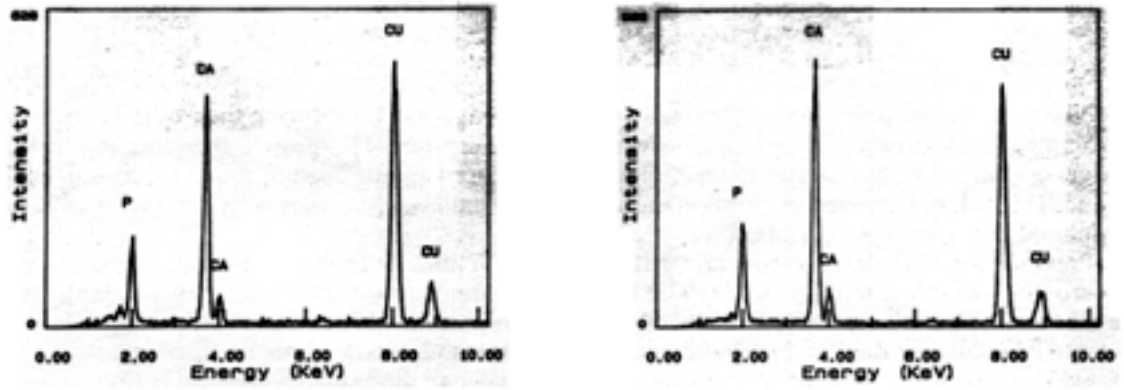

TEXT-FIG. 5. Energy Dispersive Spectrometry (EDS) X-ray spectra taken in A, polycrystalline and B, single crystal regions found in Text-figure 4. Note copper peaks are created by the copper grid used to support the apatite crystals. Both spectra exhibit the presence of phosphorus and calcium in the crystallites in the ratio expected for apatite, (hydrogen, carbon, oxygen and fluorine are not detectable with our EDS system).

(and thus at a different time) than the smaller crystallites. It appears that they were produced by crystallization of fluorapatite from saturated liquid solution, where an aqueous medium has intruded into the bone structure. The ionic species necessary for apatite crystallization could have come either from previous dissolution of a quantity of bone mineral or from the breakdown of organic material in the bone. Both hydroxyapatite and fluorapatite are relatively insoluble (Posner *et al.* 1963), but have a range of reactivities depending on pH, temperature, and composition of the solution (Chien and Black 1975). Bone apatite solubility could also be enhanced by the large surface areas of the crystallites, the high surface reactivities of the crystallites (Posner and Betts 1975), and time.

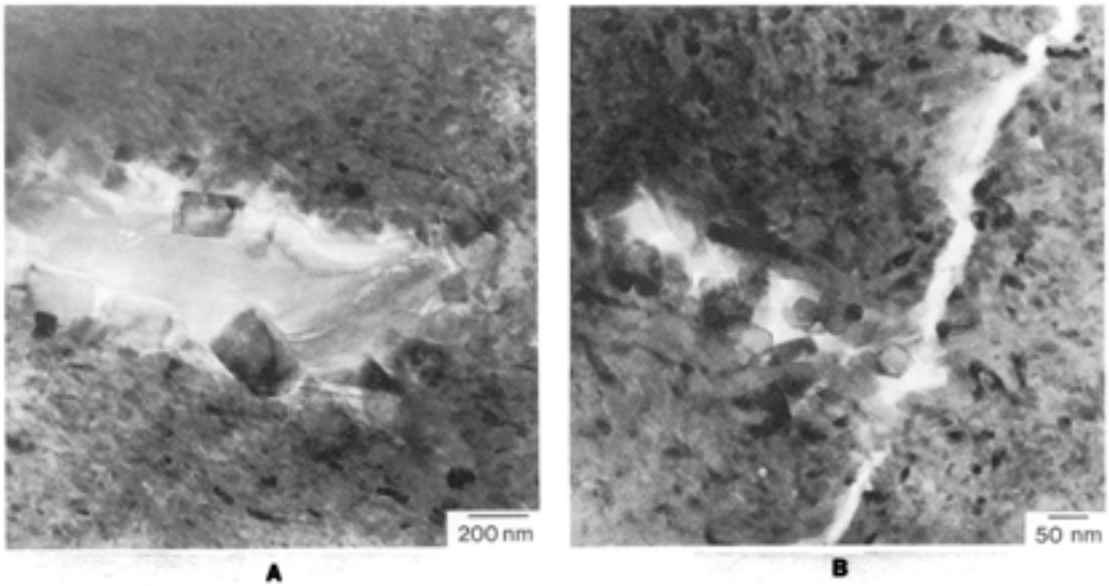

TEXT-FIG. 6. Naturally porous regions of bones showing enhanced apatite crystal growth. A, *Seismosaurus*. B, theropod dinosaur.

Non-equilibrium conditions occurring in these bones at some time during their burial may have prompted a nucleation and growth of new fluorapatite crystals. This growth therefore resulted in larger crystals, unrelated in size to the biologically produced apatite crystals found in natural living bone. The lack of preferred orientation in the larger crystallites in *Seismosaurus* and theropod bone implies a non-epitaxial nucleation.

Previous workers have noted larger-than-normal apatite crystallites in fossil bones. Using microscopic examination, Lozinski (1973) found transparent crystals of secondary fluorapatite with a tabular habit in the haversian canals of Cretaceous dinosaur ribs. Paine (1937) petrographically identified columnar dahllite in minute cracks in a Cretaceous shark tooth.

Large, platey apatite crystallites, similar to those in our dinosaur specimens, have also been grown experimentally. Koutsoukous and Nancollas (1981) grew two different forms of hydroxyapatite crystallites at 37 °C. Most of the crystallites were needle-like, but at higher pH (7·4–8·5) with a large extent of crystal growth and in the presence of chloride, larger, plate-like crystallites formed. We believe that conditions analogous to those which produced plate-like crystals in the laboratory existed in the burial environment of the *Seismosaurus* bones (the depositional setting of the theropod remains is not known). Woldegabriel and Hagan (in preparation) showed, based on mineral assemblages, that the pH of the ancient groundwater at the site was at least 9·5. There is also evidence that fluoride (similar in size, charge and bone affinity to chloride) was abundant in that groundwater, which is confirmed by its present abundance in *Seismosaurus* bone. Finally, it is thought that the strata and fossils in the *Seismosaurus* region were subjected to burial temperatures of < 60 °C (Woldegabriel and Hagan 1990, in preparation).

CONCLUSIONS

Comparing fossil to modern bone inorganic microstructure yields unique information relating to diagenesis and palaeobiology. TEM has allowed direct visual examination of the ultra- and microstructures of *Seismosaurus*, theropod dinosaur, and mammoth bones as well as modern

crocodile bone. Electron diffraction and EDS techniques were used to study the crystallography and chemistry of the apatite crystallites (francolite plus calcium fluoride phosphate). The younger mammoth and crocodile bones are composed of fine-grained hydroxyapatite crystals dispersed in a collagen fibril matrix. In all cases the apatite crystals had a local preferred orientation with the hexagonal basal planes (0001) nearly aligned, and lying perpendicular to the long axes of the collagen fibrils (when present for comparison).

The dinosaur bones are also composed largely of fine-grained hydroxyapatite crystallites, from which the finest fraction has been removed during burial and/or decomposition of the constituent organic matter within the bone. The smaller remaining crystallites are similar in size and orientation to modern bone crystallites and can be considered original. However, TEM imaging also reveals the presence of larger-sized apatite crystals, near canals and pores, in the dinosaur bones. Their random orientation and euhedral shape suggest that they are diagenetic, and formed as a result of a nucleation and growth process rather than from continued growth of existing crystallites. There is no evidence that the larger crystallites grew at the expense of the original bone material. Thus, the original microstructure of the *Seismosaurus* and theropod bones is essentially intact, only somewhat modified by the loss of the smallest fraction of crystallites and by the addition of diagenetic minerals, including apatite, to pore spaces.

Further work is necessary to confirm the process of formation of the larger apatite crystallites, to identify their distribution in other types and ages of fossil bone, and to determine what contaminating effects the presence of diagenetic apatite may have on other fossil bone analyses such as uranium and fluorine dating.

Acknowledgements. The authors are indebted to D. C. Garcia for his assistance in preparation of the TEM specimens. We thank Roland Hagan and David Gillette for organizing interdisciplinary studies of *Seismosaurus* at Los Alamos and inspiring this research. Also, the authors express their gratitude to K. E. Sickafus and G. T. Gray III for their comments and suggestions concerning this manuscript. The second author was supported, in part, by Southwest Paleontology, Inc. and New Mexico Paleoecological Research.

REFERENCES

BROPHY, G. P. and HATCH, T. M. 1962. Recrystallization of fossil horse teeth. *American Mineralogist*, **47**, 1174–1180.

CAMERON, D. A. 1972. The ultrastructure of bone. 191–236. *In* BOURNE, G. H. (ed.). *The biochemistry and physiology of bone*. Academic Press, New York, 388 pp.

CARNOT, A. 1893. Recherches sur la composition général et la teneur en fluor des os modernes et des os fossiles des différents âges. *Annales des Mines*, **3**, 155.

CHIEN, S. H. and BLACK, C. A. 1975. The activity concept of phosphate-rock solubility. *Proceedings of the Soil Science Society of America*, **39**, 856–858.

CUSINIER, F., BRES, E. F., HEMMERLE, J., VOEGEL, J.-C. and FRANK, R. M. 1987. Transmission electron microscopy of lattice planes in human alveolar bone apatite crystals. *Calcified Tissue International*, **40**, 332–338.

DOBERENZ, A. R. and WYCKOFF, R. W. G. 1967. Fine structure in fossil collagen. *Proceedings of the National Academy of Sciences, USA*, **57**, 539–541.

EANES, E. D. 1965. Effect of fluoride on human bone apatite crystals. *Annals of the New York Academy of Sciences*, **131**, 727–736.

EDDINGTON, J. W. 1976. *Practical electron microscopy in materials science*. Van Nostrand Reinholt, 344 pp.

ENGSTROM, A. 1960. Ultrastructure of bone material. 251–261. *In* RODAHL, K., NICHOLSON, J. T. and BROWN, E. M. (eds). *Bone as a tissue*. McGraw-Hill, New York, 421 pp.

—— 1972. Aspects of the molecular structure of bone. 237–257. *In* BOURNE, G. H. (ed.). *The biochemistry and physiology of bone*. Academic Press, New York, 388 pp.

FERNANDEZ-MORAN, H. and ENGSTROM, A. 1957. Electron microscopy and x-ray diffraction of bone. *Biochimica et Biophysica Acta*, **23**, 260–264.

FITTON JACKSON, S. and RANDALL, J. T. 1956. The fine structure of bone. *Nature*, **178**, 798.

GILLETTE, D. D. 1991. *Seismosaurus halli*, gen. et sp. nov., a new sauropod dinosaur from the Morrison Formation (Upper Jurassic/Lower Cretaceous) of New Mexico, USA. *Journal of Vertebrate Paleontology*, **11**, 417–433.

JAFFE, E. B. and SHERWOOD, A. M. 1951. Physical and chemical comparison of modern and fossil tooth and bone material. *Trace Elements Memorandum Report of the United States Geological Survey*, **149**, 1–22.

KOUTSOUKOS, P. G. and NANCOLLAS, G. H. 1981. The morphology of hydroxyapatite crystals grown in aqueous solution at 37 °C. *Journal of Crystal Growth*, **55**, 369–375.

LOZINSKI, J. 1973. Rare-earth elements in fossil bones. *Rocznik Polskiego Towarzystwa Geologicznego*, **43**, 408–435.

MIDDLETON, J. 1844. On the fluorine in bones, its source and its application to the determination of the geological age of fossil bones. *Proceedings of the Geological Society, London*, **4**, 431–433.

NEUMAN, W. F. and NEUMAN, M. W. 1958. *The chemical dynamics of bone mineral*. University of Chicago Press, Chicago, 209 pp.

OSMUND, J. K. and SAWIN, H. J. 1959. Unit-cell dimensions of recent and fossil tooth apatites. *Geological Society of America Bulletin, Annual Meeting Abstracts*, **70**, 1653.

PAINE, G. 1937. Fossilization of bone. *American Journal of Science*, **234**, 148–157.

PAWLICKI, R. 1978. Methods of preparation of fossil bone samples for light and transmission electron microscopy. *Stain Technology*, **53**, 95–102.

POSNER, A. S. and BETTS, F. 1975. Synthetic amorphous calcium phosphate and its relation to bone mineral structure. *Accounts of Chemical Research*, **8**, 273–281.

—— EANES, E. D., HARPER, R. A. and ZIPKIN, I. 1963. X-ray diffraction analysis of the effect of fluoride on human bone apatite. *Archives of Oral Biology*, **8**, 549–570.

—— HARPER, R. A. and MULLER, S. A. 1965. Age changes in the crystal chemistry of bone apatite. *Annals of the New York Academy of Sciences*, **131**, 737–742.

ROBINSON, R. A. and CAMERON, D. A. 1964. Bone. 315–340. *In* KURTZ, S. M. (ed.). *Electron microscopic anatomy*. Academic Press, New York, 411 pp.

SCHWARTZ, H. L. and MANLEY, K. 1992. Geology and stratigraphy of the *Seismosaurus* locality, Sandoval County, New Mexico (USA). *New Mexico Geology*, **14**, 25–30.

SHACKLEFORD, J. M. and WYCKOFF, R. W. G. 1964. Collagen in fossil teeth and bones. *Journal of Ultrastructure Research*, **11**, 173–180.

SIMPSON, D. R. 1966. Apatite and octa-calcium phosphate: effects of carbon dioxide and halogens on formation. *Science*, **154**, 1660–1661.

TANNENBAUM, P. J. and TERMINE, J. D. 1965. Statistical analysis of the effect of fluoride on bone apatite. *Annals of the New York Academy of Sciences*, **131**, 743–750.

TOWE, K. M. 1980. Preserved organic ultrastructure: an unreliable indicator for Paleozoic amino acid biogeochemistry. 65–74. *In* HARE, P. E., HOERING, T. C. and KING, K. JR. (eds). *Biogeochemistry of amino acids*. John Wiley and Sons, London, 172 pp.

TUROSS, N., BEHRENSMEYER, A. K., EANES, E. D., FISHER, L. W. and HARE, P. E. 1989. Molecular preservation and crystallographic alterations in a weathering sequence of wildebeest bones. *Applied Geochemistry*, **4**, 261–270.

—— EYRE, D. R., HOLTROP, M. E., GLIMCHER, M. J. and HARE, P. E. 1980. Collagen in fossil bones. 53–63. *In* HARE, P. E., HOERING, T. C. and KING, K. (eds). *Biogeochemistry of amino acids*. John Wiley and Sons, London, 172 pp.

WOLDEGABRIEL, G. and HAGAN, R. 1990. Temporal and spatial relationships of diagenetic processes in the Upper Jurassic Morrison Formation, Colorado and New Mexico, and its implication to dinosaur fossils preservation. *Isochron/West*, **55**, 18–23.

WYCKOFF, R. W. G. 1972. *The biochemistry of animal fossils*. Williams and Wilkins, Baltimore, 152 pp.

—— 1980. Collagen in fossil bones. 17–22. *In* HARE, P. E., HOERING, T. C. and KING, K. (eds). *Biogeochemistry of amino acids*. John Wiley and Sons, London, 172 pp.

—— and DOBERENZ, A. R. 1965. The electron microscopy of Rancho La Brea bone. *Proceedings of the National Academy of Sciences, USA*, **53**, 230–233.

—— HOFFMAN, V. J. and MATTER, P., III. 1963. Microradiography of fossilized teeth. *Science*, **140**, 78–80.

ZIPKIN, I., POSNER, A. S. and EANES, E. D. 1962. The effect of fluoride on the x-ray diffraction pattern of the apatite of human bone. *Biochimica et Biophysica Acta*, **59**, 255–258.

THOMAS G. ZOCCO
Los Alamos National Laboratory
Materials Science and Technology Division
MSG730, Los Alamos, New Mexico 87545, USA

HILDE L. SCHWARTZ
Rt. 3, Box 93-JS
Sante Fe, New Mexico 87505
USA

Typescript received 10 March 1993
Revised typescript received 7 January 1994